In-Flight Gyro Drift Rate Calibration on the Viking Orbiters

William G. Breckenridge* and Alfred J. Treder†
Jet Propulsion Laboratory, Pasadena, Calif.

The drift rates of the attitude control gyros on the Viking Orbiters were calibrated several times in flight. The process by which these rates were estimated as functions of time is novel for a space flight project, although relatively standard estimation techniques were used. The process is described fully and the results obtained from the twelve Viking single-axis gyros are analyzed. Although the possibility was explored, no significantly repeatable function of drift rate vs time or temperature was discovered; the overall mean was found to predict drift rate with acceptable accuracy.

I. Introduction

THE two Viking Orbiters (VO), still operational in orbit around Mars, each carry two redundant Inertial Reference Units (IRU) for attitude control purposes. Each IRU consists of three rate-integrating floated gyros (Kearfott C 702565007-1), with an accelerometer and associated electronics. The gyros are used for several attitude stabilization and control modes, especially for maneuver turns, in which the unpredictability of drift rate is a major attitude error source.

The drift rate of VO gyros is required to stay within 0.54 deg/h/axis (3σ) and to be stable within 0.15 deg/h (3σ) from turn-on to turn-on over a 10-day period. It is also required to be stable within 0.075 deg/h (3σ) during any continuous period of 10 h or less. These requirements were to be met over the first half of the manufacturers' design goal of 6000 h operating lifetime. Since predictability of gyro drift rate is an important factor in inertial attitude control accuracy, several in-flight calibrations were performed. The prime goal of this study was to determine the form and parameter values of the gyro drift rate function of time. The form selected to represent this function would be at the lowest order for which the error statistics would remain within the preceding Viking requirements.

The method of in-flight calibration was to engage gyro control of attitude for an otherwise undisturbed period of 6 h or more, record the apparent positions in VO coordinates of the sun and the roll reference star as a function of time, and process these data in a Viking operations computer program called GYRDFT. The analysis method developed for this process takes advantage of continuous telemetry of both celestial and inertial attitude sensor data in gyro-referenced attitude control modes to characterize in-flight gyro drift rate as a function of time from gyro turn-on. For Viking mission purposes (maneuver turns), the calibration process was required to have 3σ accuracy of 0.065 deg/h in pitch and yaw and 0.04 deg/h in roll. Typical achieved accuracy of drift rate characterization vs time was 0.012 deg/h (3σ) for telemetry resolution of ± 0.01 deg celestial and ± 0.02 deg inertial. This accuracy could not have been obtained from the available telemetry without the kind of analytical smoothing process developed for this purpose. Characterization of in-flight drift rates showed that the best predictor of gyro drift rate for maneuver design purposes was the mean over the entire calibration period and over all in-flight calibrations. Analysis of the mean functions of drift rate vs time and of the mean values over time show that the gyros met their specifications at confidence levels better than 90%, based on the χ^2 distribution with appropriate degrees of freedom.

Analysis inputs include sets of 3-axis attitude data from celestial and inertial sensor position telemetry selected at discrete points in time over the period of calibration. The analysis process can handle an arbitrary distribution in time of such sets of data points. The other essential information for the analysis is the inertial coordinates of the vectors from the spacecraft to the sun and to the roll reference star at the attitude measurement times. Spacecraft motion along its inertial trajectory causes an apparent motion of the sun, and the nonorthogonality of the star and sun vectors causes pitch and yaw coupling into roll, both of which effects are accounted for in the drift analysis.

The GYRDFT program used to process the data computes drift rates over each succeeding data increment (approximately 3.6-min intervals as implemented for Viking) in its first pass, then in the second pass smooths the calculated rate vs time function over the entire set of data according to a Gauss-Markov model of gyro drift. The autocorrelation constant of the model is selected to control the degree of smoothing.

Gyro drift itself is a slowly changing function of time. The information from which it is calculated is quantized at the spacecraft for telemetry, and then somewhat imperfectly reconstructed in ground processing. The resolution of celestial position telemetry is different from that of inertial position telemetry, leading to different time points of telemetry data change, though both are reporting a very similar motion. The scale factors assumed for celestial and inertial telemetry are independently in error. All these factors introduce "data noise" and inaccuracy into the calculated gyro drift. The shorter the time period over which the drift is calculated, the greater the noise effects. The longer the time period used, the less information obtained on the short-term variations of gyro drift.

Two things were done to minimize the effects of data noise. The first was to use a relatively long time-constant in the Gauss-Markov model of gyro drift to provide a high degree of smoothing in the estimation process and to be consistent with the true drift behavior of the Viking hardware. The other action was to determine empirically a set of celestial sensor scale factor corrections (not estimated by GYRDFT) to correct for celestial/inertial scale factor error differences, so as to minimize the rms error of the data fit.

The next two sections develop the full analytical process and discuss the results for the Viking gyros.

Received Oct. 12, 1977; revision received March 14, 1978.

Index categories: Spacecraft Navigation, Guidance, and Flight-Path Control; Spacecraft Testing, Flight and Ground; Analytical and Numerical Methods.

*Member of Technical Staff, Guidance and Control Section.
†Senior Engineer, Guidance and Control Section.

II. Analytical Method

Reference Frames

Data for estimation of Viking gyro drift consisted of onboard celestial and inertial attitude measurements taken while the spacecraft was under gyro attitude control. Reduction of these data to net inertial motion of gyro nulls requires the use of five coordinate systems:

1) The inertial reference frame (XYZ), in which are defined the unit vectors $\hat{h}$ and $\hat{s}$ from the spacecraft to its celestial reference bodies.

2) The celestial coordinate system (ABC), defined by $\hat{h}$ and $\hat{s}$, which represents the nominal attitude of the spacecraft celestial sensors when locked on their reference bodies.

3) The nominal spacecraft body coordinates (xyz), defined with respect to ABC by the orientations on the spacecraft of the celestial sensor nulls.

4) The actual spacecraft body-fixed axes ($x'y'z'$) which deviate from nominal xyz due to attitude control limit cycling, inertial reference drift, etc.

5) The gyro null (GN) coordinate system defined with respect to $x'y'z'$ by the integrated rate outputs of the gyros.

In the XYZ inertial reference frame for Viking, $\hat{h}$ is the unit vector from spacecraft to sun and $\hat{s}$ is the unit vector from spacecraft to a reference star.

The ABC celestial reference frame is defined by the transformation matrix T_A^X from XYZ to ABC:

$$T_A^X = \begin{bmatrix} [(\hat{h}\times\hat{s})\times\hat{h}]^T/|\hat{h}\times\hat{s}| \\ [\hat{h}\times\hat{s}]^T/|\hat{h}\times\hat{s}| \\ [\hat{h}]^T \end{bmatrix} = \begin{bmatrix} \hat{A}^T \\ \hat{B}^T \\ \hat{C}^T \end{bmatrix} = [\hat{X}\ \hat{Y}\ \hat{Z}]_{ABC} \qquad (1)$$
$$XYZ$$

In the ABC system, the C axis is toward the sun, the B axis is perpendicular to the sun/star plane, and the A axis completes the set. An important quantity for later use is the angle between the sun and star vectors:

$$\beta = \cos^{-1}(\hat{h}\cdot\hat{s}) \qquad (2)$$

The nominal body coordinates (xyz) are defined for Viking as $\hat{z} = -\hat{C}$, and $\hat{x}$ located 225 deg from $\hat{A}$ in rotation about $\hat{C}$, so that the transformation T_x^A from ABC to xyz is:

$$T_x^A = \begin{bmatrix} \cos\alpha_x & \sin\alpha_x & 0 \\ \sin\alpha_x & -\cos\alpha_x & 0 \\ 0 & 0 & -1 \end{bmatrix} \text{ where } \alpha_x = 225 \text{ deg} \qquad (3)$$

Pitch, yaw, and roll (p, y, r) control axes nominally correspond to x,y,z, respectively. The deviation of $x'y'z'$ actual body axes from their nominal orientation can be represented by an ordered sequence of control axis rotations: pitch by θ_p, yaw by θ_y, and roll by θ_r. Thus, the transformation $T_{x'}^x$ from xyz to $x'y'z'$ is:

$$T_{x'}^x = [\theta_r]_3\ [\theta_y]_2\ [\theta_p]_1 \qquad (4)$$

where $[\theta]_i$ is a 3×3 transformation matrix corresponding to a rotation of angle θ about axis i.

The deviation from nominal attitude causes nonzero angle error signals ($\emptyset_p, \emptyset_y, \emptyset_r$) to be generated by the pitch and yaw sun sensors and roll star sensor. Calibration of the celestial sensors may have determined null offset (δ) and scale factor (k) corrections to be applied to the telemetered angles ($\emptyset_p', \emptyset_y', \emptyset_r'$) so that

$$\emptyset_i = \delta_i + (1+k_i)\emptyset_i' \qquad i=p,y,r \qquad (5)$$

The relationship of these $\emptyset_i$'s to the θ_i's ($i=p,y,r$) is approximated (to the second order) for the Viking configuration by

$$\theta_r = \emptyset_r(1-\emptyset_b\cot\beta) - (\emptyset_p\cos\alpha_x + \emptyset_y\sin\alpha_x)\cdot(\emptyset_b/2+\cot\beta) - (\emptyset_p\emptyset_y/2)$$
$$\text{where}\quad \emptyset_b = \emptyset_p\sin\alpha_x - \emptyset_y\cos\alpha_x$$
$$\theta_p = \emptyset_p - \theta_r\cdot\emptyset_y$$
$$\theta_y = \emptyset_y + \theta_r\cdot\emptyset_p \qquad (6)$$

Coincident with the celestial sensor signals defining $x'y'z'$, the strapdown pitch, yaw, and roll gyros output the angles ψ_p, ψ_y, ψ_r, indicating the attitude of the spacecraft ($x'y'z'$) with respect to the gyro null coordinate system (GN). The GN coordinate system corresponds to the spacecraft axis orientation when the ψ's are all zero, assuming that it got to its current position by a pitch, yaw, roll sequence of turns from null, and can get back to GN by the reverse sequence. Thus the transformation $T_{x'}^{GN}$ from gyro null to $x'y'z'$ is defined:

$$T_{x'}^{GN} = [\psi_r]_3\ [\psi_y]_2\ [\psi_p]_1 \qquad (7)$$

The assumption regarding turn sequence for the gyros is required because the GN coordinate system is not unique. With single-axis gyros, any number of turn sequences can terminate with all ψ's zero, and each will give a different GN because of the noncommutativity (NC) of turns. This ambiguity can be removed only by a detailed analysis of the time history of the ψ's. Since provision for such analysis will not be made in this development, the GN coordinate system just described will drift with time according to the accumulated NC turn errors. Although this NC drift is indistinguishable from true gyro drift rate, it was an insignificant source of error for Viking. As an example calculation, if each axis had the same control deadband width d (radians) and limit cycle period c (time units), the worst case NC drift rate would be d^2/c (radians/time unit) per axis. For Viking flight data, worst case was on the order of 0.001 deg/h, an order of magnitude less than other drift error sources.

The transformations given in Eqs. (1-7) are used to define the inertial orientation of the gyro null coordinate system:

$$T_{GN}^X = [T_{x'}^{GN}]^{-1}\,[T_{x'}^x]\,[T_x^A]\,[T_A^X] \qquad (8)$$

where

T_{GN}^X = transformation from inertial reference to gyro null coordinates.

Drift Angle

Gyro drift is the change in the gyro null position with time. Figure 1 shows a typical sample of spacecraft attitude telemetry during a gyro drift calibration sequence. [Specifically, these data consist of converted and corrected telemetry selected every 3½ min from a higher rate data stream, covering the period approximately 2-4 h after gyro turn-on for the prime inertial reference unit (IRU 1) on the second Viking spacecraft (Viking II)]. A rough idea of attitude drift rates relative to celestial references can be obtained by noting the long-term change in the celestial sensor signals. Gyro drift is one part of this attitude drift.

The previous section gave the method for determining gyro null position at any time from measurement of the celestial sensor and gyro error signals. The drift between two times is determined from the gyro null positions at those times[1]:

$$[D]_{t_i t_j} = [T_{GN}^X]_{t_j}\,[T_{GN}^X]_{t_i}^{-1} \qquad (9)$$

where $[D]_{t_i t_j}$ = transformation matrix corresponding to drift between t_i and t_j. The drift may be represented as a vector, $\bar{d} = d\hat{d}$, where $\hat{d}$ is the axis of rotation from $GN(t_i)$ to $GN(t_j)$ and d = angle of rotation from $GN(t_i)$ to $GN(t_j)$.

These are evaluated by first defining

$$\bar{d}' = \begin{bmatrix} D_{23} - D_{32} \\ D_{31} - D_{13} \\ D_{12} - D_{21} \end{bmatrix} \tag{10}$$

where subscripts indicate elements of the matrix D.

Given the preceding vector $\bar{d}'$, the following can be shown:

$$d = \sin^{-1}(|\bar{d}'|/2), \qquad \hat{d} = \bar{d}'/|\bar{d}'| \tag{11}$$

Measurement Accuracy

The error in determining the gyro null position is determined by the errors in the sensor angle measurements. Let a vector of pitch and yaw sun sensors, roll star sensor, and pitch, yaw, and roll gyro measurement errors be $\bar{\epsilon}$ with covariance Λ_ϵ. Then, for small sensor angles, a first-order representation of the error, $\bar{e}$, in GN, expressed as a rotation vector in GN coordinates is:

$$\bar{e} = \begin{bmatrix} 1 & 0 & 0 & -1 & 0 & 0 \\ 0 & 1 & 0 & 0 & -1 & 0 \\ -\cot\beta\cos\alpha_x & -\cot\beta\sin\alpha_x & 1 & 0 & 0 & -1 \end{bmatrix} \bar{\epsilon} = E\bar{\epsilon} \tag{12}$$

$$\operatorname{cov}(\bar{e}) = E\Lambda_\epsilon E^T \tag{13}$$

The error $\bar{\delta}$ in the drift between t_i and t_j is:

$$\bar{\delta} = \bar{e}_j - [D]_{t_i t_j}\bar{e}_i$$

Assuming that over the time period t_i to t_j: $\bar{\epsilon}_i$ and $\bar{\epsilon}_j$ are statistically independent, implying that they are primarily data noise errors; $\Lambda_{\epsilon_i} = \Lambda_{\epsilon_j}$, the errors are stationary; $[D]_{t_i t_j} \simeq I$, drift angles are small; and $E_i \simeq E_j$, no large change in β,

then

$$\operatorname{cov}(\bar{\delta}) \simeq \operatorname{cov}(e_j) + \operatorname{cov}(e_i) = 2E\Lambda_\epsilon E^T \tag{14}$$

These assumptions and approximations are consistent with the Viking gyro drift calibration procedures used.

The gyro drift rate estimates are made on each axis independently, ignoring correlations between axes, and therefore the 1σ measurement accuracy of the kth axis drift is defined as the scalar

$$\sigma_k = \sqrt{[\operatorname{cov}(\bar{e})]_{kk}} \tag{15}$$

Gyro Drift Rate Estimates

Gyro drift occurs simultaneously in all three single-axis gyros and the cumulative drift angle is a function of the behavior of all three axes. The drift angle measurement noise is also correlated between axes. However, for small drift angles and reasonably stable drift rates, each axis of drift may be investigated independently with no significant degradation of accuracy. The remainder of this section will treat only a single axis of drift, using the kth component d_k of the vector $\bar{d}$ as the drift angle, and σ_k as the corresponding rms measurement accuracy. The subscript k will be dropped for simplicity of notation.

Three estimates are computed – two based on adjacent data points and the third filtered and smoothed over the whole set of data points.

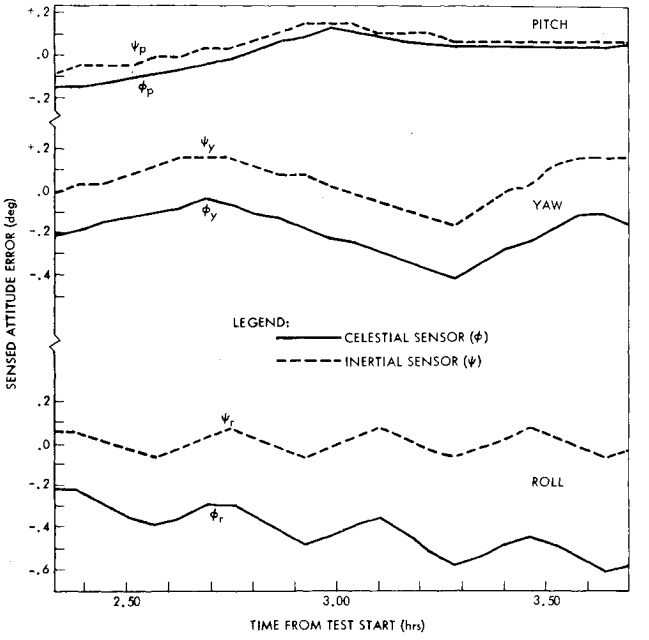

Fig. 1 Typical attitude telemetry during gyro drift rate calibration.

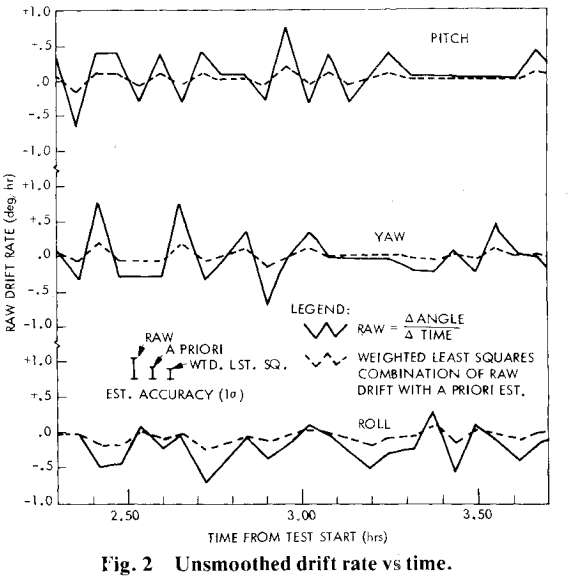

Fig. 2 Unsmoothed drift rate vs time.

Computed Drift Rate.

The average drift rate between t_{i-1} and t_i may be computed directly as

$$w_i = d(t_{i-1}, t_i)/(t_i - t_{i-1})$$

with a variance of

$$\sigma_{w_i}^2 = 2\sigma^2/(t_i - t_{i-1})^2$$

This value of w_i may be very noisy if the interval between data points is short.

Estimated Drift Rate

The same data points may be used in an estimate (minimum variance) that includes any a priori information about the drift rate. Because Viking calibrations were separated in time much farther than the anticipated autocorrelation time, the a priori information was the set of design parameters

$$\left.\begin{aligned} w_0 &= 0.00 \text{ deg/h} \\ \sigma_{w_0} &= 0.18 \text{ deg/h} \end{aligned}\right\} \text{a priori design values for Viking}$$

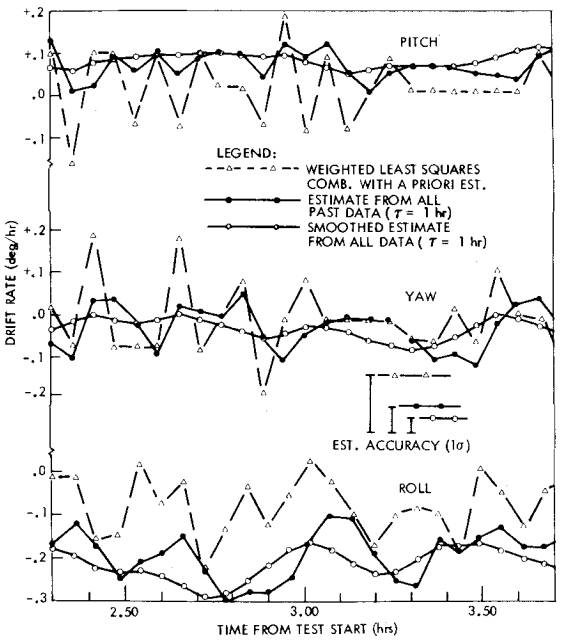

Fig. 3 Effect of processing level on drift rate estimate.

The minimum variance estimate is then:

$$\sigma^2_{w_i} = \left[\frac{1}{\sigma^2_{w_0}} + \frac{(t_i - t_{i-1})^2}{2\sigma^2}\right]^{-1} \tag{16}$$

$$w_i = \sigma^2_{w_i} \cdot \left[\frac{2\sigma^2}{(t_i - t_{i-1})^2}\right]^{-1} \cdot d(t_{i-1}, t_i)/(t_i - t_{i-1})$$

$$= \frac{\sigma^2_{w_0} \cdot d(t_{i-1}, t_i)/(t_i - t_{i-1})}{\sigma^2_{w_0} + 2[\sigma/(t_i - t_{i-1})]^2} \tag{17}$$

This estimate is less noisy than the computed drift rate and is biased toward the a priori value. Figure 2 compares these types of drift rate estimates, which were made from the data of Fig. 1. Note that the weighted least squares (minimum variance) estimates are biased toward zero with respect to the raw average estimates.

Filtered and Smoothed Drift Rate

This estimator processes the drift angle measurements as cumulative from the first point of the data set, so that d_i will represent $d(t_i, t_0)$. The drift angle is modeled as if drift rate were a random process.

$$a_i = a_{i-1} + w_i \Delta t_i = \text{drift angle at } t_i$$

$$w_i = \rho_i w_{i-1} + q_i \quad = \text{drift rate at } t_i$$

where $\Delta t_i = t_i - t_{i-1}$, ρ is $\exp(-\Delta t_i/\tau)$ for Gauss-Markov process, τ is the time constant of the random Gauss-Markov process, q_i = random perturbation to drift rate, and $Q_i = (1 - \rho_i^2) \cdot \sigma^2_{w_0}$, variance of q_i. The drift rate w_i is the average drift rate over the interval $i-1$ to i, and the perturbations to w are assumed to occur at data point times.

The data processing consists of two passes; first a forward estimation consisting of prediction and minimum variance estimation steps for each data point, then a backward pass to perform the smoothing,[2] i.e., to get the best estimate at each point based on all data in the set, not just the earlier data as in the first pass. Figure 3 compares the results of the forward estimation and backward smoothing passes with the weighted least-squares estimate from Fig. 2 (note the scale difference between the two figures). Appendix A describes a recursive algorithm to perform this data processing.

Selection of Autocorrelation Time Constant (τ)

The typical drift rate functions of Figs. 2 and 3 illustrate the effects of data noise and its suppression by the smoothing process. There are two primary causes for this noise: 1) the scale factors of the celestial and inertial telemetry channels are independently in error, and 2) the telemetry is digital, with different resolution for celestial and inertial sensors. The latter characteristic alone causes ± 0.5 deg/h worst-case error in the raw drift rate (Fig. 2) due to telemetry resolution of ± 0.01 deg celestial vs ± 0.02 deg inertial, calculated over an interval of 0.06 h. The phase walk of the digital signals forces this worst case to occur regularly in the telemetry data stream.

Figure 3 illustrates the reduction in data noise obtained with Gauss-Markov smoothing when the autocorrelation time constant (τ) is 1.0 h. Figure 4 shows the effect on the same data for $\tau = 1$, 10, and 100 h (note vertical scale change). The noise is evident, though greatly suppressed, even at $\tau = 100$. The estimation accuracy shown in Fig. 4 for each value of τ is the true value for the drift rate process which has that autocorrelation constant. If the process is Gauss-Markov and τ for smoothing is selected smaller than true τ, estimation accuracy will be worse than shown in the figure, since not all noise will be properly damped. If τ is selected too large, accuracy may suffer if significant components of the actual process are suppressed. The autocorrelation time of Viking gyros was expected to be on the order of 1000 h; this can be calculated from the performance requirements:

$$\tau = \frac{2(\text{time interval})}{-\ln\left(1 - \dfrac{\text{stability variance over time interval}}{\text{overall variance}}\right)}$$

The 10-h continuous stability requirement of 0.075 deg/h (3σ), compared to the overall drift rate requirement of 0.54 deg/h (3σ) gives $\tau = 1027$ h.

Adjustment of Relative Scale Factor

As previously mentioned, the mismatch of scale factor errors between celestial and inertial sensor telemetry creates data noise. The GYRDFT program that computes gyro drift rates for Viking has two features which help reduce the effects of this error source:

1) An input variable, *SF*, which is used internally to rescale the celestial telemetry input data for each axis according to the formula:

$$(\text{internal value}) = (1 + SF) \cdot (\text{input value})$$

2) An output of the mean and standard deviation of the difference between the raw [d in Eq. (11)] and smoothed estimates of total drift angle.

Figure 5 shows this drift angle error as a function of *SF* for the first calibration of VO2 IRU 1; the minimum of the curve is a "best" value of *SF* for this set of data. The upper part of Fig. 5 shows the effect of *SF* on estimated drift rate; as could be expected, the estimate is directly proportional to this rescaling factor, with a maximum effectiveness of 1.0. (In the example, the roll drift rate estimate changes 10% for every 0.10 change in *SF*.)

The minimum variance estimate of *SF*, by the preceding criterion, provides correction of the celestial sensor telemetry scale factor relative to that of the inertial sensor. Because this minimum variance of angle error depends on the time history of attitude deviations, different sets of data on the same control axis will produce different minimum variance estimates of *SF*, each of which is "best" for the data set and none of which is the correct rescaling term in the absolute sense. In addition, any selection of *SF* on such a basis is subject to the absolute error of the inertial sensor telemetry. However, in the absence of sufficiently accurate independent information on the absolute celestial scale factor, the

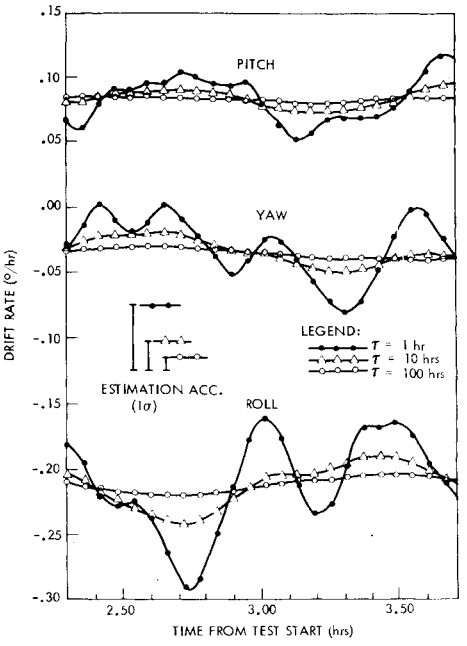

Fig. 4 Smoothed drift rate vs autocorrelation constant.

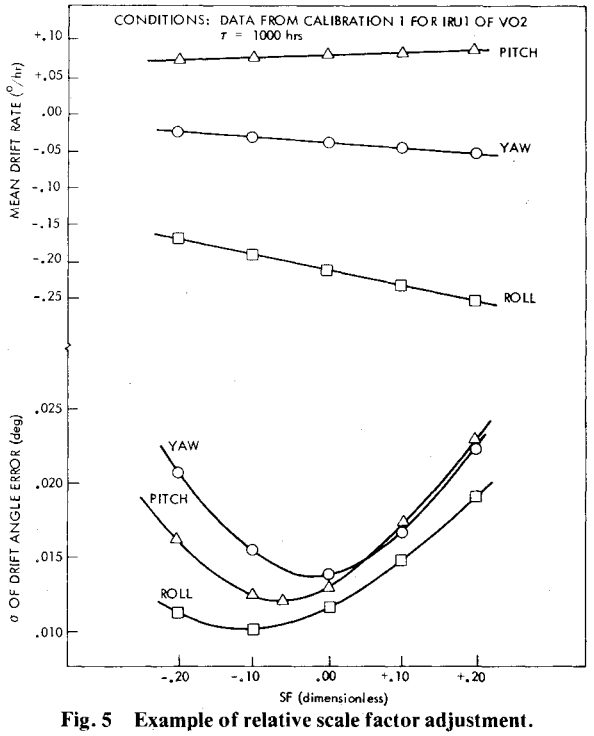

Fig. 5 Example of relative scale factor adjustment.

minimum noise criterion offers the likelihood of improved results. All final Viking results were computed with both the best *SF* for each calibration sample and the average of such *SF* values; the overall mean drift rate is the same with either method within 1%.

III. In-Flight Calibration Results

In-flight calibration of Viking gyros was performed three times on the prime IRU and once on the secondary for each spacecraft during trans-Mars cruise, followed by one calibration of each prime IRU in Mars orbit prior to separation of the Lander from the Orbiter. The in-orbit calibration for Viking I was on the roll gyro only (the difference between this and an all-axis calibration is discussed in Appendix B). A similar roll-only calibration of IRU-2 on

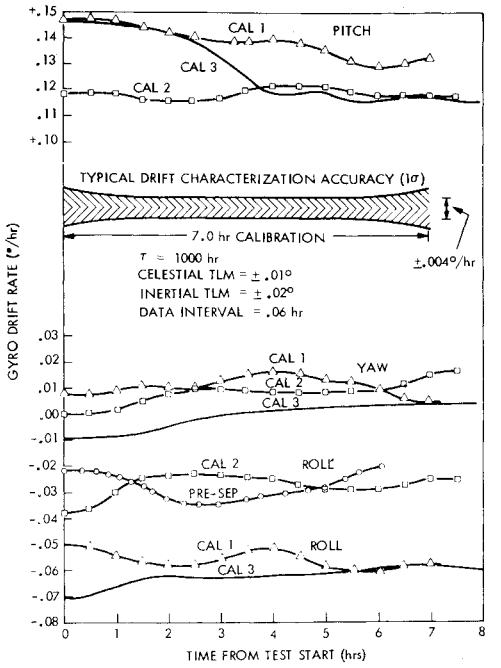

Fig. 6 Results of in-flight gyro drift rate calibrations for V01 IRU1.

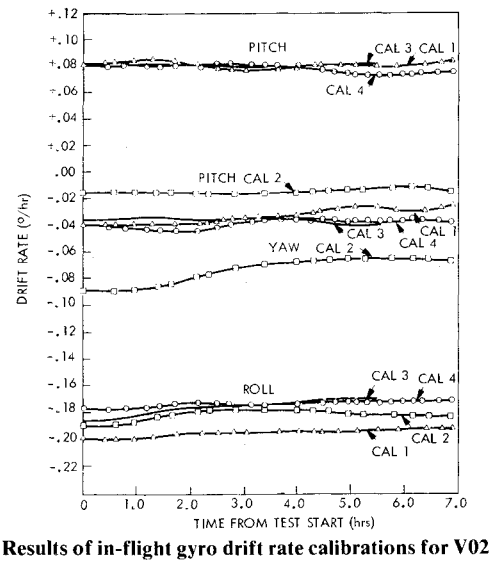

Fig. 7 Results of in-flight gyro drift rate calibrations for V02 IRU1.

Viking II was performed after the unit became prime on that spacecraft. All told, twelve gyros were calibrated under in-flight zero-*g* conditions, one to four times per gyro, at 1-5 month intervals, during the prime Viking mission (Aug. 1975 to Nov. 1976).

Figures 6 and 7 characterize per-axis gyro drift rate as a function of time for every calibration of IRU-1 on spacecraft 1 and on spacecraft 2, respectively. The autocorrelation time constant τ for the smoothing process was 1000 h, and the celestial telemetry rescaling factor (*SF*) used for each axis was the average of the minimum drift noise *SF*s determined for that axis in the first three calibrations. Figure 6 also has a plot of typical drift rate estimation error as a function of time location within the data set. This estimation error function is typical of the Fig. 7 plots as well.

The variation of drift rate with time that can be seen in Figs. 6 and 7 is gyro behavior, not residual data noise. If there were higher frequency components of drift rate variation, which is possible, they were unavoidably suppressed by the smoothing process. However, the smooth changes which can be seen are significant with respect to the estimation accuracy, and to that accuracy characterize the true behavior of gyro

Table 1 Results of VO '75 gyro drift rate calibrations during the prime mission

Item	Mean gyro drift rate (deg/h)					
	Ground calibrations	In-flight calibrations				Overall in-flight calibrations
		#1	#2	#3	#4	
			VO 1, IRU 1			
Date		10/30/75	3/18/76	5/25/76	7/1/76	
Pitch	+0.074	+0.1398	+0.1209	+0.1270	N/A	+0.1292
Yaw	−0.009	+0.0123	+0.0085	−0.0013	N/A	+0.0065
Roll	−0.021	−0.0548	−0.0275	−0.0621	−0.0294	−0.0434
			VO 1, IRU 2			
Date		3/22/76	N/A	N/A	N/A	
Pitch	−0.025	−0.198				+0.198
Yaw	+0.037	+0.010				+0.010
Roll	−0.031	+0.022				+0.022
			VO 2, IRU 1			
Date		10/23/75	3/15/76	5/12/76	8/26/76	
Pitch	+0.050	+0.0809	−0.0148	+0.0796	+0.0779	+0.0559
Yaw	−0.022	−0.0341	−0.0725	−0.0355	−0.0392	−0.0453
Roll	−0.104	−0.1926	−0.1838	−0.1778	−0.1756	−0.1824
			VO 2, IRU 2			
Date		3/26/76	9/4/76	N/A	N/A	
Pitch	+0.027	−0.003	N/A			−0.003
Yaw	+0.097	+0.1405	N/A			+0.1405
Roll	−0.024	+0.0243	−0.033			−0.005

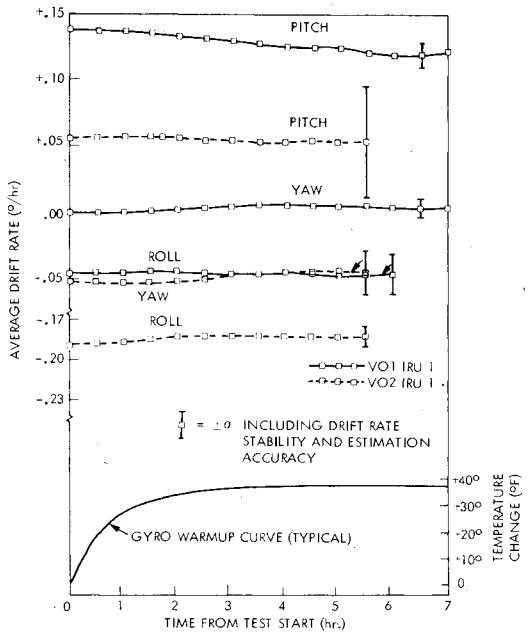

Fig. 8 Average gyro drift rate vs time.

drift during periods of continuous operation. Turn-on-to-turn-on variation is evidenced by the differences between calibrations of the same gyro at the same relative time for test start.

In order to sort out the repeatable function of gyro drift vs time, values were averaged over all calibrations at the same time from turn-on and plotted in Fig. 8. Also shown in this figure is an error bar for turn-on-to-turn-on stability and estimation accuracy for each gyro, and a typical gyro warmup curve. In this comparison it is difficult to assert anything but random behavior as a function of time or temperature. For predicting future behavior of Viking gyro drift, the zeroth order function (overall average) is clearly sufficient.

Table 1 lists the dates of occurrence and drift rate mean values over time for each in-flight calibration and the mean over all such calibrations, for the period of the Viking prime mission. Also included for comparison are the mean ground calibration results. There has been very good agreement (within 0.07 deg/h except for one instance) among all measurements of any given gyro, including comparison of in-flight with ground calibration. The worst observed variation of smoothed drift rate within any calibration period of continuous operation was 0.065 deg/h peak-to-peak; most variations were less than half that, and thus the 0.075 deg/h (3σ) short-term stability requirement was well met. Taking those gyros calibrated more than once as seven samples of the class of Viking gyros, and allowing for the different number of measurements of each gyro, the average turn-on-to-turn-on stability of these gyros was 0.15 deg/h (3σ) at the 90% confidence level. Taking the overall mean drift rates of all twelve gyros as samples of overall drift deviation from design mean value (zero), the group has 3σ of 0.51 deg/h at about 96% confidence. For the limited number of measurements, these results give good confirmation of in-flight gyro performance meeting its requirements.

IV. Summary

A recursive algorithm for calculating smoothed gyro drift rate as a function of time has been derived. The use of this algorithm for determining Viking gyro drift rates has been discussed and the results analyzed. No repeatable function of gyro drift rate vs time or temperature could be demonstrated at any useful level of significance. The best predictor of drift rate value for Viking gyros was found to be the overall mean value. All measures of actual variation about this mean value showed that these gyros met their a priori requirements at high levels of confidence.

Appendix A: Recursive Estimation Algorithm

We have chosen to estimate a parameter vector p consisting of rate w, angle a, and bias e_0. The bias is included as an estimated parameter, since the measurement error at the initial point offsets all subsequent computed drift angles (d_i).

The initial estimate value p_0^e and its covariance P_0^e are stipulated at time t_0 of the first data point:

$$p_0^e = [0, \quad 0, \quad 0]^T$$

$$P_0^e = \begin{bmatrix} \sigma_{w_0}^2 & 0 & 0 \\ 0 & 0 & 0 \\ 0 & 0 & \sigma^2 \end{bmatrix}$$

The recursive steps for each subsequent data point are as follows:

1) Get next data point (at t_i) and compute $d_i = d(t_i, t_0)$.
2) Predict-extrapolate previous point to t_i:
   a) Degrade rate knowledge for the new interval

$$\rho_i = \exp[-(t_i - t_{i-1})/\tau]$$

$$p''_{i-1} = \begin{bmatrix} \rho_i & 0 & 0 \\ 0 & 1 & 0 \\ 0 & 0 & 1 \end{bmatrix} p^e_{i-1} = R_i p^e_{i-1}$$

$$P''_{i-1} = R_i P^e_{i-1} R_i^T + \begin{bmatrix} Q_i & 0 & 0 \\ 0 & 0 & 0 \\ 0 & 0 & 0 \end{bmatrix}$$

where $Q_i = (1 - \rho_i^2)\sigma_{w_0}^2$

   b) Extrapolate to t_i by $\Delta t_i = (t_i - t_{i-1})$

$$p'_i = \begin{bmatrix} 1 & 0 & 0 \\ \Delta t_i & 1 & 0 \\ 0 & 0 & 1 \end{bmatrix} p''_{i-1} = T_i p''_{i-1}$$

$$P'_i = T_i P''_{i-1} T_i^T$$

   c) Compute the backward mapping matrix for the current instance (t_i), to be used later for smoothing:

$$B_i = P^e_{i-1} (T_i R_i)^T P'^{-1}_i$$

3) Estimate p_i using drift angle measurement d_i

$$d_i = [0 \;\; 1 \;\; -1] p_i + n = A p_i + n$$

where the measurement noise $n = N(0, \sigma)$.

$$p^e_i = p'_i + P'_i A^T (A P'_i A^T + \sigma^2)^{-1} (d_i - A p'_i)$$

$$P^e_i = P'_i - P'_i A^T (A P'_i A^T + \sigma^2)^{-1} A P'_i$$

4) Save for the smoothing pass: p^e_i, P^e_i, p'_i, P'_i, and B_i.
5) Repeat from step 1 until last data point is processed.

The second (backward) processing pass is for smoothing. The last (nth) value of the estimate is already based on all data so

$$p^*_n = p^e_n \quad \text{and} \quad P^*_n = P^e_n$$

These are used to start ($i = n$) the backward recursion that produces the smoothed estimates.

$$p^*_{i-1} = p^e_{i-1} + B_i (p^*_i - p'_i)$$

$$P^*_{i-1} = P^e_{i-1} + B_i (P^*_i - P'_i) B_i^T$$

$$i \leftarrow i - 1$$

Continue the backward recursion until $i = 0$. Each estimate, p^*_i and P^*_i, is the desired estimate based on all data.

A third pass is made forward through the data to provide a printout of the three estimates in proper time order and to evaluate the mean and standard deviation of the residuals, $d_i - (a^*_i - e^*_0)$, from the smoothed estimate.

Appendix B: Variations for Roll Inertial

The drift of the roll gyro can be calibrated when the spacecraft is in the roll inertial mode, i.e., the pitch and yaw axes are controlled by the sun sensors and the roll axis (around the sun-line) by the roll gyro. In this mode, there are variations in the coordinate systems used and we are concerned with only one drift angle – roll.

The nominal spacecraft motion in this mode is to rotate about the orbital pole ($\hat{OP} \simeq \hat{h} \times \hat{h}$) with zero rate component along roll ($-\hat{h}$ for Viking). On the other hand, the celestial coordinate (ABC) has a rate component along roll unless the reference star vector, $\hat{s} = \pm \hat{OP}$. To account for this motion of ABC, the roll angle measurement used is the roll angle from the orbital pole to the gyro null defined as

$$RM = PA + \theta_r - \psi_r$$

PA = roll angle from $\hat{OP}$ to $\hat{A}$

$$= \tan^{-1}[(\hat{OP} \cdot \hat{B})/(\hat{OP} \cdot A)], \text{ for Viking}$$

and the roll drift is:

$$d(t_i, t_j) = RM(t_j) - RM(t_i)$$

Acknowledgment

The work described in this paper was performed by the Control and Energy Conversion Division of the Jet Propulsion Laboratory, California Institute of Technology, under the sponsorship of the Viking 1975 Project, managed by NASA Langley Research Center.

References

[1] Goldstein, Herbert, *Classical Mechanics*, Addison-Wesley, Mass., 1950 (especially Chap. 4 on the kinematics of rigid body motion).

[2] Sage, A.P., and Melsa, J.L., *Estimation Theory with Applications to Communications and Control*, McGraw-Hill, New York, 1971, Chaps. 7 and 8.